Joint inversion of ReMi dispersion curves and refraction travel times using particle swarm optimization algorithm

A. Zarean[1*] and R. Poormirzaee[2]

1. *Department of Civil Enginnering, Shabestar Research Branch, Islamic Azad University, Shabestar, Iran*
2. *Department of Mining and Material Engineering, Urmia University of Technology, Urmia, Iran*

Abstract

Shear-wave velocity (V_S) is an important parameter used for site characterization in geotechnical engineering. However, dispersion curve inversion is challenging for most inversion methods due to its high non-linearity and mix-determined trait. In order to overcome these problems, in this study, a joint inversion strategy is proposed based on the particle swarm optimization (PSO) algorithm. The seismic data considered for designing the objects are the Rayleigh wave dispersion curve and seismic refraction travel time. For joint inversion, the objective functions are combined into a single function. The proposed algorithm is tested on two synthetic datasets, and also on an experimental dataset. The synthetic models demonstrate that the joint inversion of Rayleigh wave and travel time return a more accurate estimation of V_S in comparison with the single inversion Rayleigh wave dispersion curves. To prove the applicability of the proposed method, we apply it in a sample site in the city of Tabriz located in the NW of Iran. For a real dataset, we use refraction microtremor (ReMi) as a passive method for getting the Rayleigh wave dispersion curves. Using the PSO joint inversion, a three-layer subsurface model was delineated.The results obtained for the synthetic datasets and field dataset show that the proposed joint inversion method significantly reduces the uncertainties in the inverted models, and improves the revelation of boundaries.

Keywords: *Shear Wave, Joint Inversion, Remi, Particle Swarm Optimization, Travel Time.*

1. Introduction

Seismic surveying techniques provide relevant data regarding soil behavior at a very low strain level for large portions of soil, tested in an undisturbed state using the procedures that are time- and cost-effective [1]. Shallow shear-wave velocity (V_S) has long been recognized as a key factor in variable ground-motion amplification and site response in sedimentary basins [2]. The velocity profiles together with the depth of the basement below the sediments are the useful data used in geotechnical studies for the correct construction of buildings [3]. The V_S structure is important in site-effect studies and geotechnical engineering, but it is quite difficult and expensive to derive it from the conventional geophysical techniques [4]. The current techniques of estimating shallow shear-wave velocities for assessment of earthquake site responses are too costly for use at most construction sites [5].

The refraction microtremor (ReMi) method [5] is a passive-source multi-channel method that uses a linear array configuration. This method provides effective and efficient means to obtain the general information about large volumes of the sub-surface in one dimension per setup, where the appropriate setup length is related to the desired depth of investigation [6]. ReMi is based on obtaining the dispersion curve for the Rayleigh waves, but in this case, using the ambient seismic noise or microtremor. For the processing procedure, as for the other surface wave methods, after construction of the dispersion curves, the next step is the inversion of the dispersion curve to obtain a single V_S profile. The inversion stage

in processing the ReMi data, due to its non-linearity and multi-dimensionality, is an important issue to achieve a reliable V_S profile.

Surface wave inversion is strongly non-linear, ill-posed, and mix-determined, and this leads to strong solution non-uniqueness, as evidenced by several authors [1]. In order to overcome these problems, constraining the interpretation, and decreasing the uncertainty in estimating the structures was proposed, which is based upon the PSO algorithm. Inverting the recorded data sets separately may lead to incorrect interpretation of an underground structure, i.e. for an underground model with a high-velocity layer overlying a low velocity layer, neither refraction nor reflection seismic alone is able to resolve the parameters of the low-velocity layer [7]. The information required for the water table, bed rock, and layer interface can be obtained using the refraction seismic, whereas dispersion curves do not give any information about the number of layers, while the refraction travel times, in principle, could [8]. Therefore, it is possible, by integration of the surface waves and refraction travel time, to reduce the intrinsic weakness of each method.

For joint inversion by particle swarm optimization (PSO) algorithm, we used the global criterion method, in which all misfit functions (i.e. objective functions) were combined to form a single function. By finding the global minimum of the misfit function, the best solution to a problem could be obtained. PSO algorithm is one of the global optimization methods that belong to a group of metaheuristic searching algorithms. In geophysical surveys, several significant PSO applications have recently been emerged. Fernández Martínez et al. [9] have presented the application of a whole family of PSO algorithms to analyze and solve a VES inverse problem associated with a seawater intrusion in a coastal aquifer in southern Spain. Pekşen et al. [10] have inverted the self-potential (SP) data by the application of PSO algorithm. Poormirzaee et al. [11] have proposed the seismic travel time inversion scheme based on the particle swarm optimization technique. Recently, Zarean et al. [12] have presented the application of mutation-based PSO algorithms to analyze the surface wave dispersion curves using the microtremor records.

The proposed joint inversion algorithm was written and processed in MATLAB, and tested on the synthetic datasets. Finally, the reliability of the PSO joint inversion was investigated in a sample site in Tabriz located in the NW of Iran in order to study the site effect. The results obtained for both the synthetic and real datasets were compared with the single PSO inversion of ReMi data, and also with a multi-objective optimization algorithm, non-dominated sorting genetic algorithm-II (NSGA-II).

2. Methodology
2.1. Particle Swarm Optimization (PSO)

PSO is a stochastic evolutionary computation optimization technique used in many engineering fields. It is inspired by the social behavior of the individuals (called particles) in groups in nature like a flock (swarm) of birds searching for food [13]. This algorithm searches the space for an objective function by adjusting the trajectories of individual agents, called particles, as these trajectories form piecewise paths in a quasi-stochastic manner [14]. The particles move toward promising regions of the search space by exploiting information springing from their own experience during the search as well as the experience of other particles. For this purpose, a separate memory was used, where each particle stores the best position (x_i^*) it has ever visited in the search space. The best position of each particle experience the other comprised ones, and then the best position, which belongs to a minimum of misfit function, selected as the global best (g^*). This procedure (i.e. finding x_i^*, g^*) was repeated for a certain iteration. Finally, the best global g^* was determined as the optimum solution. The movement of particles was schematically represented in Figure 1.
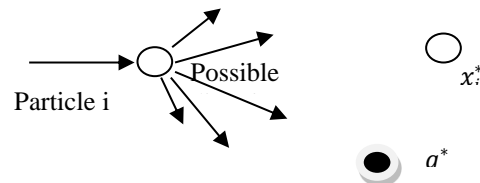

Figure 1. Schematic representation of motion of a particle in PSO, moving towards global best g^* and current best x_i^* for each particle [14].

Particle swarm consists of a swarm of particles, each moving or flying through the search space according to the velocity update Eq.1 [13]. The velocity of each particle was modified iteratively by its personal best position, and the best position was found by the particles in its neighborhood. v_i is the velocity of the ith particle in the swarm, x_i is the particle position, x_i^* denotes the personal best position, and g^* is the best position found by particles in its neighborhood.

$$v_i^{t+1} = v_i^t + \alpha\epsilon_1\odot\left(g^* - x_i^t\right) + \beta\epsilon_2\odot\left(x_i^* - x_i^t\right) \tag{1}$$

In Eq. 1, ϵ_1 and ϵ_2 are two random vectors and each entry takes a value between 0 and 1. The Hadamard product of the two matrices $u \odot v$ is defined as the entry-wise product. The parameters α and β are the learning parameters or acceleration constants, which can typically be taken as, say, $\alpha \approx \beta \approx 2$ [14].

The initial locations of all particles should distribute relatively uniformly so that they can sample over most regions, which are especially important in multimodal problems. The initial velocity of a particle can be taken as 0, i.e. $v_i^{t=0} = 0$. The new position can then be updated by Eq. 2 [14].

$$x_i^{t+1} = x_i^t + v_i^{t+1} \tag{2}$$

A number of variations have been proposed on the original PSO to overcome its shortcomings and drawbacks such as slow convergence and wandering near the global minimum in the final stage of the search. One of the most notable steps in these formulations is the introduction of an inertia weight by Shi and Eberhart [15]. An inertia term (i.e. static inertia weight), $\omega \in (0,1)$, was introduced into the original PSO velocity rule, as follows:

$$v_i^{t+1} = \omega v_i^t + \alpha \epsilon_1 \odot (g^* - x_i^t) + \beta \epsilon_2 \odot (x_i^* - x_i^t) \tag{3}$$

So long as $\omega \in (0,1)$, Eq. 3 helps the particles forget their lower-quality past positions in order to be more affected by the higher-quality information of late, which seems to make more sense conceptually [16].

For $\omega, \alpha,$ and β, there are several popular parameter sets in the literature (Table 1). Another notable recent variation in the original PSO algorithm is the introduction of the so-called constriction factor by [17]. This method introduces a constriction factor $\chi \in (0,1)$ into the original velocity rule (i.e. Eq. 1), which has the effect of reducing the velocity of the particles as the search progresses, and thereby contracting the overall swarm diameter. This, in turn, results in a progressively smaller domain being searched [18]. Applying a constriction factor into PSO improves the convergence of the particles (Eq. 4). The other parameters used in different studies are listed in Table 1.

$$v_i^{t+1} = \chi [v_i^t + \alpha \epsilon_1 \odot (g^* - x_i^t) + \beta \epsilon_2 \odot (x_i^* - x_i^t)] \tag{4}$$

Using the constriction factor seems to be superior to the introduction of the inertia term (for more information, see [16]).

Another feature of the PSO algorithm is the velocity clamping, which is important for its improvement. Eberhart and Kennedy have introduced velocity clamping, which helps particles take reasonably sized steps in order to comb through the search space rather than bouncing almost excessively [16].

Like other evolutionary algorithms, the difficulty in escaping from the local optimum still exists in PSO. Some researchers have used the mutation operator to make the PSO break away from the local optimum. The PSO algorithm with mutation operator not only has great advantages of convergence property but also can avoid the premature convergence problem [19].

Table 1. Proposed PSO parameter sets in different references.

No. Set	PSO parameters				Reference
	α	β	χ	ω	
1	1.300	2.800	0.7298	-	Schutte and Groenwold [20]
2	2.050	2.050	0.7290	-	Evers [16]
3	0.948	2.041	-	0.729	Carlisle and Dozier [21]
4	1.700	1.700	-	0.600	Trelea [22]
5	1.494	1.494	-	0.729	Clerc and Kennedy [23]
6	2.000	1.800	-	0.800	Fernández Martínez et al. [18]

2.2. Refraction Microtremor (Remi) And Seismic Refraction Techniques

The ReMi technique is a cheap and quick "passive" geophysical technique. It is based upon the ambient noise measurements that are carried out with seismic arrays to obtain information on the surface wave velocity dispersion. Urban conditions such as the existing underground facilities and ambient noise due to cultural activity restrict the general application of the conventional geophysical techniques [24]. The ReMi method combines the urban utility and ease of microtremor array techniques with the operational simplicity of the spectral analysis of the surface wave (SASW) technique and the shallow accuracy of the multi-channel analysis of the surface wave (MASW) technique. As for the SASW technique, ReMi is based upon obtaining the dispersion curve of the Rayleigh waves, but in this case, the ambient seismic noise or microtremor is used.

Configurations of 12-48 single vertical, 8-12 Hz exploration geophones can give surface-wave phase velocities at frequencies as low as 2 Hz and as high as 26 Hz. This range is appropriate for constraining the shear velocity profiles from the surface to 100 m depth [5].

After Louei [5], the reliability and accuracy of the ReMi method has been investigated in different case studies. Rucker [6] has applied the ReMi shear-wave technique for the geotechnical characterizations, and several geotechnical applications have been shown in his publication. Scott et al. [25] have performed measurement of the shear-wave velocity to 30 m depth (V_{S30}) for the hazard assessment of Reno basin. They were successful in obtaining the detailed shallow shear-wave velocity transect across an entire urban basin with a minimum effort. Coccia et al. [26] have used the ReMi technique for determining the 1D shear-wave velocity in a landslide area, and have concluded that in marginally stable slope areas, the ReMi method can provide the data needed for calculating the shear-wave velocity vertical profiles down to a depth of few tens of meters. This issue can be achieved even using an array shorter than the commonly recommended minimum value of 100 m. Panzera and Lombardo [27] have successfully used the ReMi and MASW techniques to investigate the dynamic properties of the main lithotypes outcropping in the Siracusa region and their relationships with the local seismic response. Poormirzaee and Hamidzadeh [28] applied the ReMi data to study the structure of V_S in urban areas, while using other active seismic methods was limited.

The seismic refraction surveying method uses the seismic energy that returns to the surface after traveling through the ground along the refracted ray paths. The first arrival of the seismic energy at a detector offset from a seismic source represents either a direct ray or a refracted ray [29]. On the local scale, the refraction surveys are widely used in the foundation studies on the construction sites to derive estimates of the depth to the rock head beneath a cover of the superficial material. Refraction surveys find wide applications in the exploration programs for underground water supplies in sedimentary sequences, often employed in conjunction with the electrical resistivity methods.

In general, the travel time t_n of a ray, critically refracted along the top surface of the nth layer, is given by the following relation:

$$t_n = \frac{x}{v_n} + \sum_{i=1}^{n-1} \frac{2 z_i \cos \theta_{in}}{v_i} \tag{5}$$

Where

$$\theta_{in} = \sin^{-1}(v_i / v_n)$$

In Eq. 5, x is the offset distance from shot point, v is the velocity of layer, z is the depth of refractor, and $\sin \theta = v_1 / v_2$ is the Snell's Law [29].

2.3. Joint inversion of Rayleigh wave and refraction travel time by PSO

The Rayleigh wave dispersion curves and refraction travel times are jointly inverted through a procedure based on the PSO technique. The main goal of the proposed algorithm is to improve the reconstruction of the subsurface structure by exploiting the complementary information attainable by the Rayleigh wave dispersion and refraction travel times. The Rayleigh wave dispersion inversion procedure was performed using the fundamental mode.

The most important parameters that influence the Rayleigh wave propagation are the shear-wave velocity (V_S) and layer thickness, while density (ρ) and P-wave velocity (V_P) play a minor role [30]. On the other hand, the refraction travel time depends on the longitudinal velocity and thickness. In order to obtain accurate results, in the joint inversion procedure, it was decided to link V_P and V_S by means of the Poisson ratio (σ). In this way, in general, a wide range of Poisson values $[0.1, 0.48]$ is allowed for each layer. Of course, a suitable range of Poisson values depend on the studied area, which can be determined by the primary information. Using Eq. 6 and the above Poisson values, a straight equation was obtained (Eq. 6). For each particle (i.e. the model), the V_P and V_S values were checked to detect the V_P/V_S ratio. If this ratio exceeds the imposed limits, the algorithm for satisfying Eq. 6 generates new random values for V_P and V_S.

$$v_p = v_s \left(\frac{\sqrt{1-\sigma}}{\sqrt{\frac{1}{2} - \sigma}} \right) \tag{6}$$

$$1.5 < \frac{v_p}{v_s} < 5 \tag{7}$$

Also the parameter density was fixed according to the classical Gardner et al [31] empirical V_P–ρ relationship:

$$\rho = \log(0.23 + (kVp)^{0.25}) \tag{8}$$

Where $K = 1 / 0.3048$ is a constant to convert feet to meter.

For the joint inversion of ReMi and seismic refraction data, the summation of the root mean square (RMS) error was considered as the objective function (OBF). In order to solve the forward modeling, and estimate the theoretical dispersion curve, the code based on the matrix algorithm developed by Herrmann [32] was used. The root mean square misfit between the observed and calculated values for velocity was defined as the objective function (OBF_1) according to the following equation:

$$OBF_1 = \sqrt{\frac{\sum_{j=1}^{n_p}(v^{obs} - v^{cal})^2}{n_p}} \qquad (9)$$

where n_p is the number of samples, v^{obs} is the observed phase velocity, and v^{cal} is the calculated one.

Also the forward algorithm used in the inversion is based on a 1D ray-tracing for the P-wave travel times. The root mean square misfit between the observed and calculated refraction travel times are defined as the object function (OBF_2), according to the following equation:

$$OBF_2 = \sqrt{\frac{\sum_{j=1}^{n_p}(t^{obs} - t^{cal})^2}{n_p}} \qquad (10)$$

where n_p is the number of points, t^{obs} is the observed travel time, and t^{cal} is the calculated travel time. Also, for the seismic refraction data, the forward algorithm used in the inversion is based on a 1D ray-tracing for the P-wave travel times.

In the joint inversion procedure, the elements of the objective function can have different physical dimensions and various orders of magnitude. Thus to have stable results, normalization is needed [7]. For normalization, the values for the parameters in the objective function are divided into its observed values (Eq. 11).

$$OBF = \sqrt{\frac{(\frac{\sum_{j=1}^{n_p}(X^{obs} - X^{cal})}{X^{obs}})^2}{n_p}} \qquad (11)$$

where x^{obs} is the observed value, and x^{cal} is the calculated one. The general flowchart of the PSO joint inversion algorithm is shown in Figure 2. We investigated this algorithm in some synthetic and real datasets.

2.4. Synthetic Dataset

In order to test the PSO joint inversion algorithm, and evaluate its performance, we considered two synthetic models (A and B). Also for an efficient study of the proposed joint inversion algorithm (i.e. PSO joint Inv.), the obtained V_S profile was compared with the estimated V_S profile of PSO single inversion of ReMi data (i.e. PSO Inv.), and also by the non-dominated sorting genetic algorithm (NSGA-II). In the PSO single inversion approach [33], only the ReMi data was inverted. NSGA-II, Proposed by Deb et al. [34], is a modified version of the non-dominated sorting genetic algorithm (NSGA), proposed by Srinivas and Deb [35]. This algorithm, as a multi-objective optimization algorithm, has been investigated in many literatures [36].

To investigate the PSO joint inversion algorithm, we first considered the 4-layer synthetic model reported in Table 2 (model A). Also the particle and maximum number of iterations were selected to be 80 and 50, respectively. The adopted model was designed in order to reproduce a typical hidden-layer case, which is clearly prone to erroneous refraction travel time interpretation. The dispersion curve and the estimated travel time values are showed in Figures 3a and 3b. Also the mean results obtained for different inversion algorithms for model A are shown in Table 3 and Figure 3c.

The PSO joint inversion method is probed by a four-layer model (model B). Table 4 shows model B and the search space used for inversion. The dispersion curve and the estimated travel time values are showed in Figures 4a and 4b. The mean results obtained for inversion in model B are shown in Table 5 and Figure 4c.

2.5. Field Dataset

To further explore the applicability of the PSO joint inversion algorithm described above, the ReMi and seismic refraction data was acquired in the city of Tabriz in the NW of Iran (Figure 5). Then the dataset was reanalyzed in the present study using the PSO joint inversion approach. The data was collected in a profile line. In this study, the ReMi and seismic refraction method was performed using an OYO 24-channal seismograph and 4.5Hz and 28 Hz geophones with a receiver spacing of 5 m. Unfiltered 17 second records were collected at the studied site. Also fourteen records were gathered. The ReMi data processing consisted of three steps: 1) preliminary detection of surface waves 2) extracting the dispersion curve 3) inversion of the dispersion curve. In this study, the module Pickwnin/SW of the commercial software package SeisImager v.3.1 [37] for detection of surface waves and getting dispersion curve was used (Figure 6).
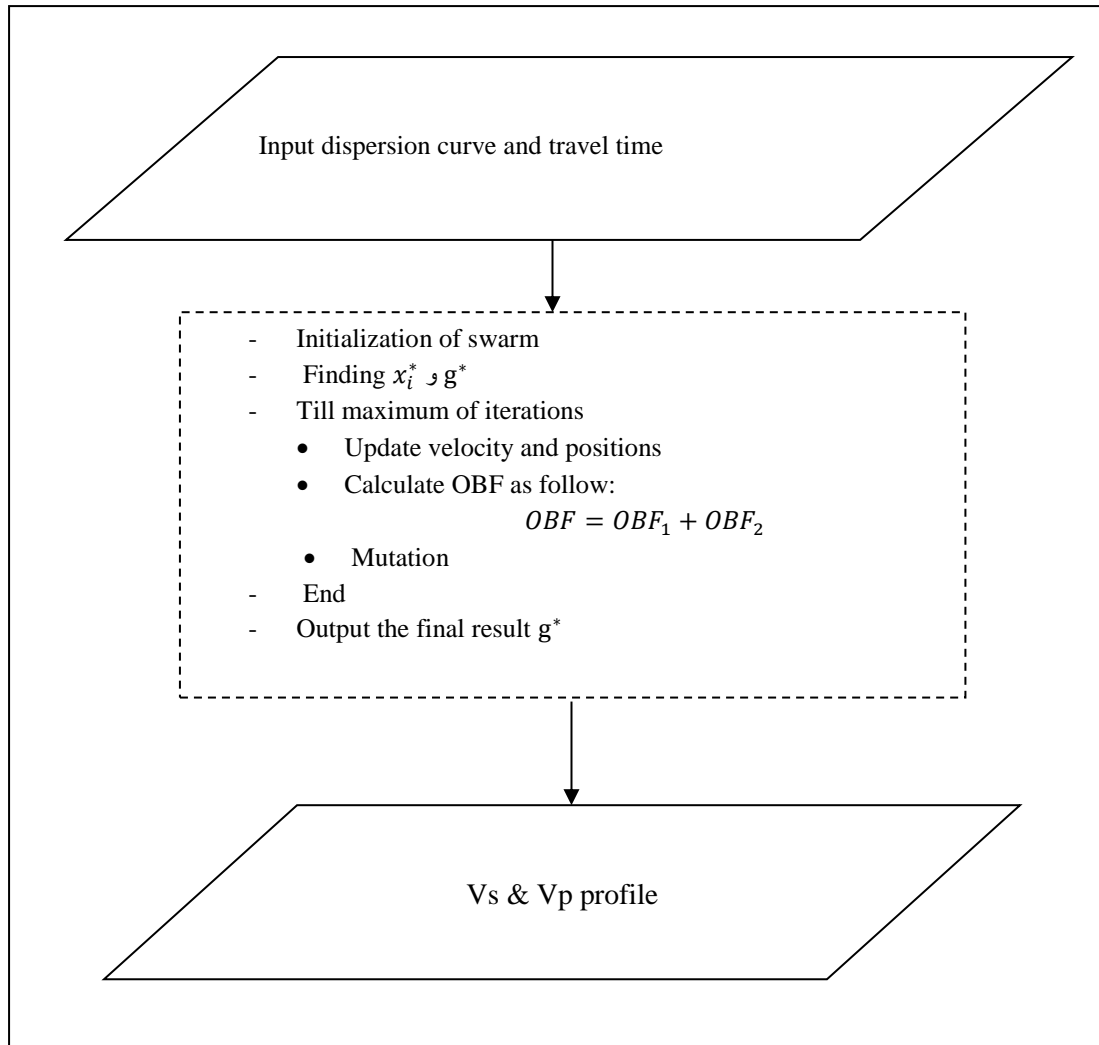
Figure 2. PSO joint inversion algorithm to invert dispersion curve and travel time dataset.

Table 2. Parameters of synthetic model A and search space.

Layer number	V_S (m/s)	V_P (m/s)	H (m)	Search space		
				V_P (m/s)	V_S (m/s)	H (m)
1	190	400	4	200-600	90-300	2-6
2	370	700	5	350-1050	150-550	2-7
3	220	430	5	200-600	100-300	2-7
4	700	1250	half space	700-2000	350-1000	-

Table 3. Mean model obtained from model A by different inversion algorithms.

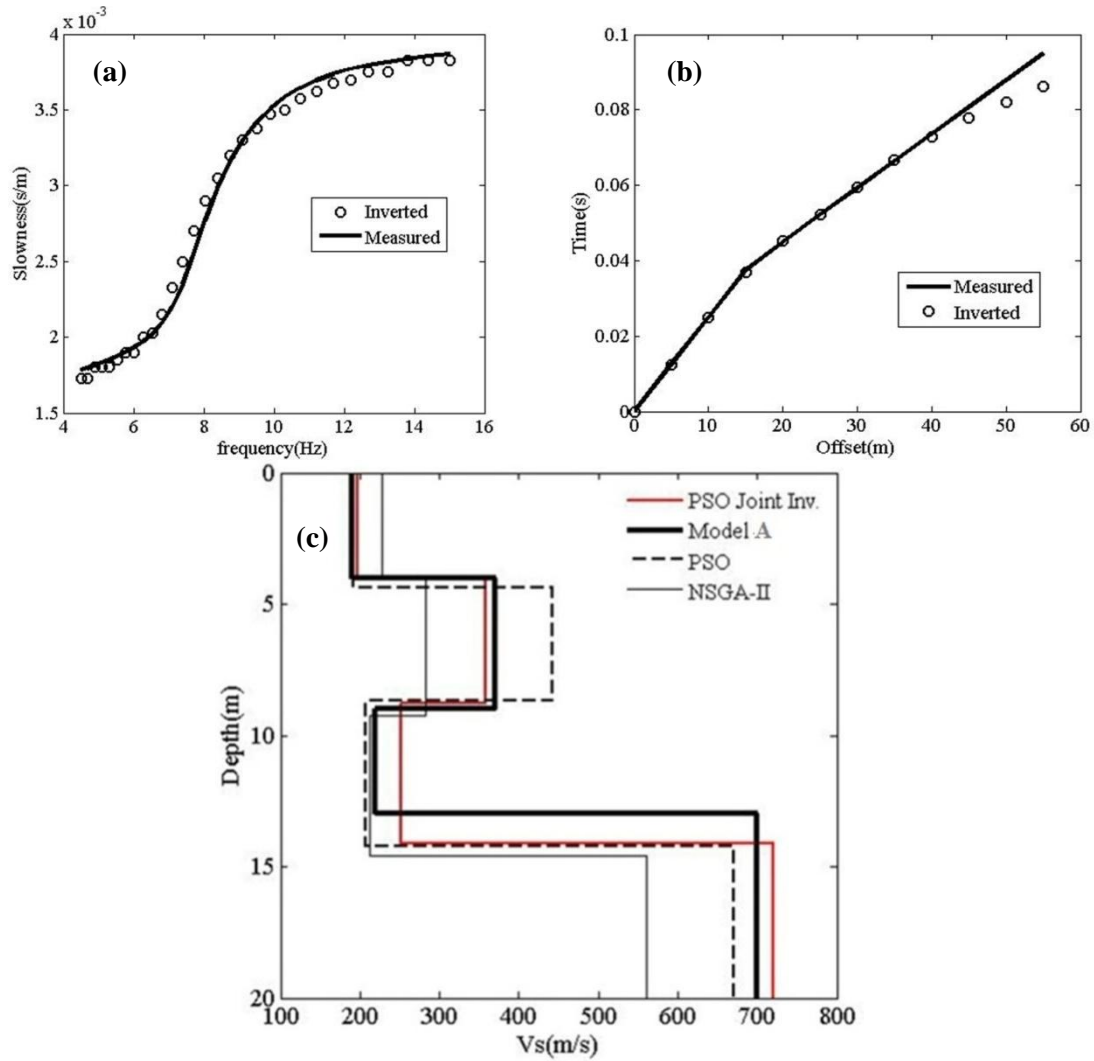| Parameters	PSO Inv. (ReMi data)	PSO joint Inv.	NSGA-II
V_S1 (m/s)	192	197	227
V_S2 (m/s)	442	358	283
V_S3 (m/s)	208	251	212
V_S4 (m/s)	670	720	560
H1 (m)	4.4	4	4.05
H2 (m)	4.3	4.8	5.2
H3 (m)	5.5	5.3	5.4
V_P1 (m/s)	472	386	401
V_P2 (m/s)	668	664	705
V_P3 (m/s)	500	522	350
V_P4 (m/s)	1112	1119	965

Figure 3. a) Inversion of dispersion curve using PSO joint inversion for model A b) Inversion of travel times using PSO joint inversion for model A V_S profile using PSO joint Inv., PSO, and NSGA-II .

Table 4. Parameters of synthetic model B and search space.

Layer number	V_S (m/s)	V_P (m/s)	H (m)	Search space		
				V_P (m/s)	V_S (m/s)	H (m)
1	285	700	3	350-1050	142-427	1-5
2	163	400	2	200-600	80-244	1-3
3	600	1470	10	700-2100	300-900	5-15
4	1328	2300	half space	1150-3400	664-1900	-

Table 5. Mean model obtained from model B.

Parameters	PSO Inv. (ReMi data)	PSO joint Inv.	NSGA-II
V_S1 (m/s)	290	298	270
V_S2 (m/s)	187	197	214
V_S3 (m/s)	642	628	661
V_S4 (m/s)	947	1326	1332
V_P1 (m/s)	539	610	661
V_P2 (m/s)	402	486	527
V_P3 (m/s)	1420	1134	1611
V_P4 (m/s)	2158	2195	1304
H1 (m)	2.6	2.8	3
H2 (m)	2.4	1.8	3
H3 (m)	9.1	9.6	9.6
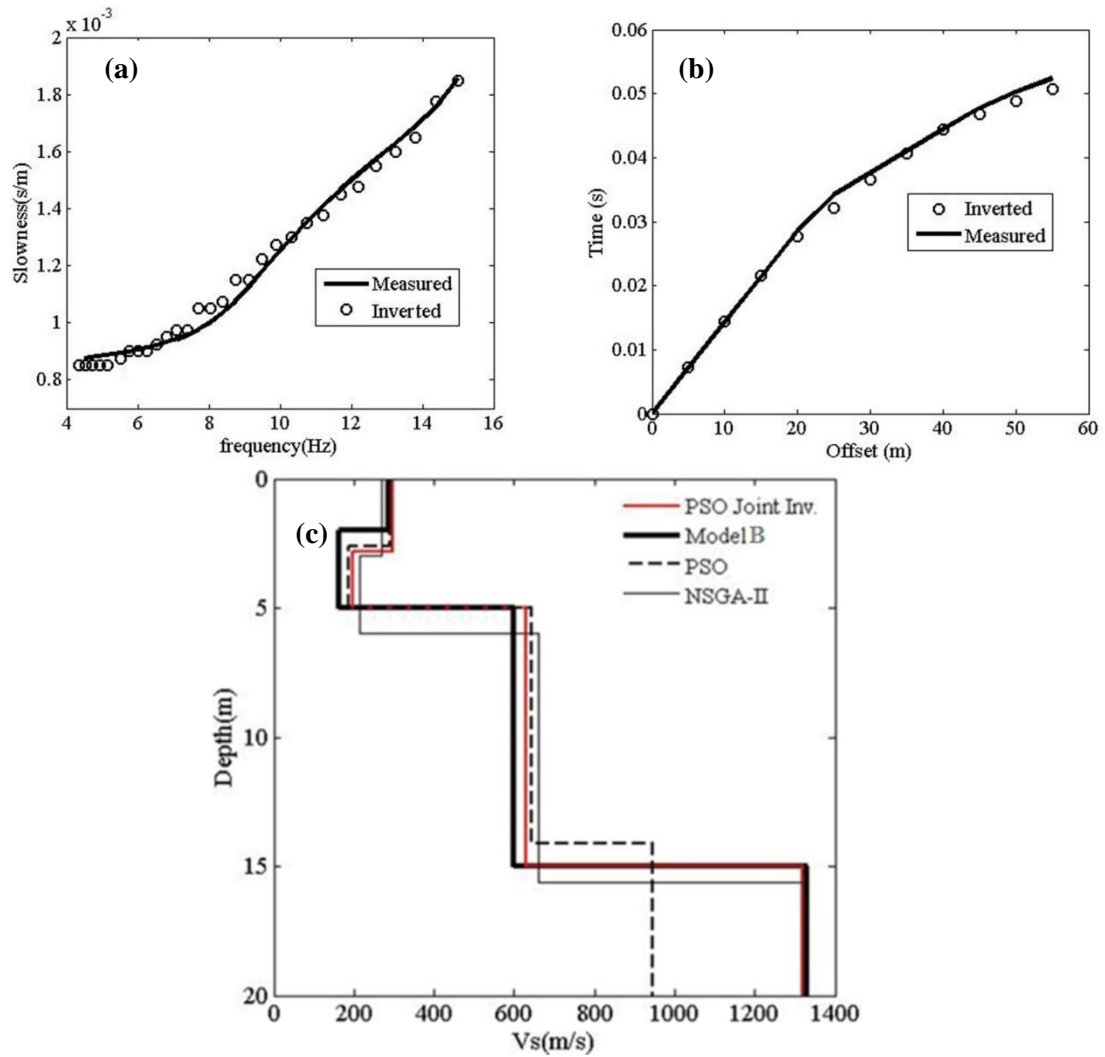
Figure 4. a) Inversion of dispersion curve using PSO joint inversion for model B, b) Inversion of travel times using PSO joint inversion for model B, and c) V_S profile of model B using PSO joint Inv., PSO, and NSGA-II.
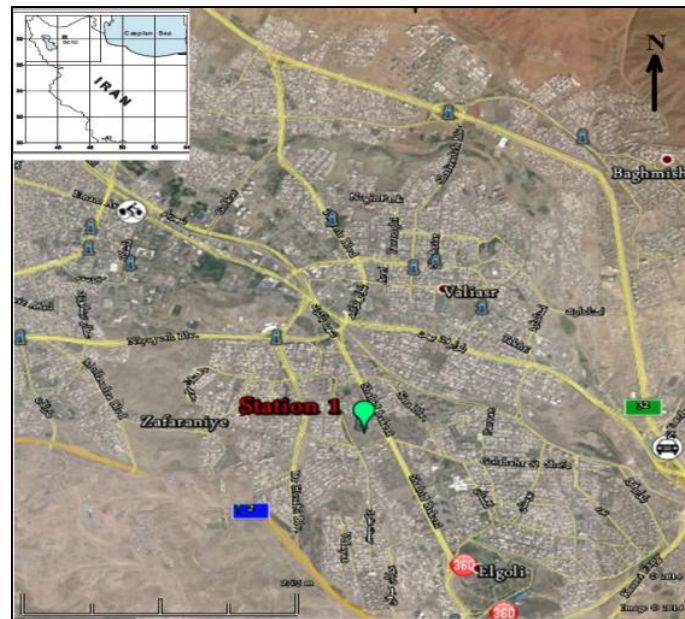

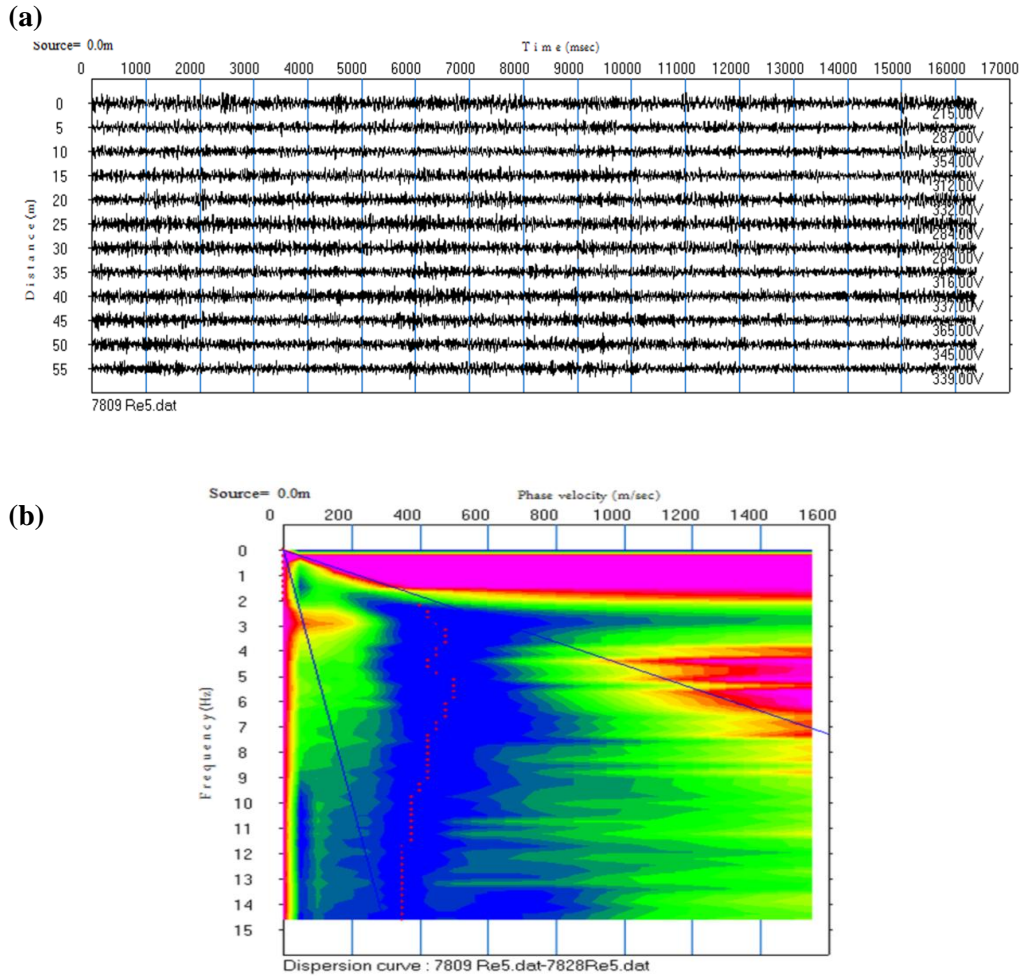**Figure 5. Location of studied area in Tabriz (NW of Iran).**

(a)

(b)

Figure 6. Field dataset a) A sample record of ReMi data b) Dispersion curve (red points, maximum amplitudes on phase velocity-frequency plot).

Also the sledge-hammer (12 kg) source was used to generate the seismic signals for the seismic refraction data. In case of the seismic refraction, both the forward and reverse shootings were carried out along with the profile over a lateral distance of 115 m. The seismic results obtained indicated that the area was composed of two main layers that were nearly lateral (Figure 7).

For the joint inversion procedure, a line with a 55 m length was selected (Figure 8). Similar to the inverse strategy of synthetic cases, we considered V_S, V_P, and thickness (H) of the layers, as the variables (Table 6). After a number of runs and considering different models, by paying attention to the observed dispersion curve, a 3-layer model

was adopted. The results obtained for the V_S profile were shown in Figure 9, in which there was a low velocity in depth (about 5 m). The results shown in Table 7 and Figures 9 and 10, have a good correlation with the geology. The upper layer made up of soil consisting of alluvium and sandy clay, and the second layer made up of clay soil and Tuff also there is water table in depth about 5m [38]. Moreover, the results obtained showed the V_P profile in detail, and detected a thin layer with a velocity of about 650 m/s (Figure 10). Moreover, the PSO joint inversion compared with the PSO inversion and NSGA-II approach.

Table 6. Search space for PSO joint inversion of field dataset.

Layer number	Search space		
	thickness(m)	P-wave velocity (m/s)	S-wave velocity (m/s)
1	2-7	400- 700	150- 450
2	1-5	450- 900	200- 550
3	-	800-1600	350-750

Table 7. Mean model obtained from field dataset.

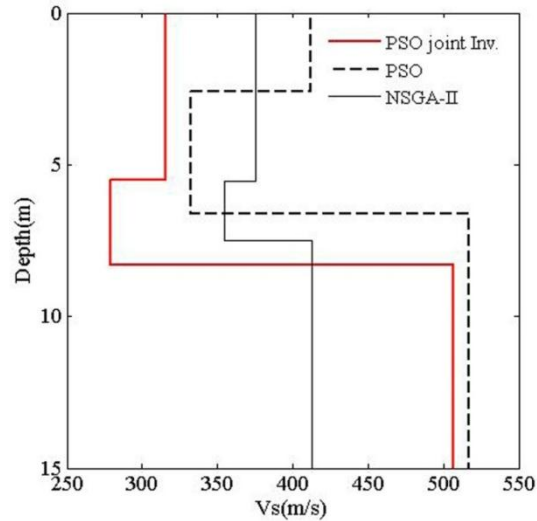| parameters	PSO Joint Inv.	NSGA-II	PSO
H1 (m)	5.5	5.53	2.6
H2 (m)	2.8	1.98	4
V_P1 (m/s)	507	523	680
V_P2 (m/s)	657	509	473
V_P3 (m/s)	1455	1114	1350
V_S1 (m/s)	316	385	412
V_S2 (m/s)	280	373	332
V_S3 (m/s)	512	405	517
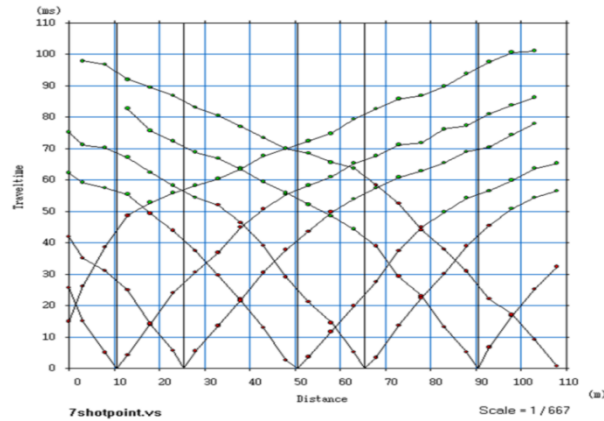
Figure 7. Time-distance plot of refraction field dataset.
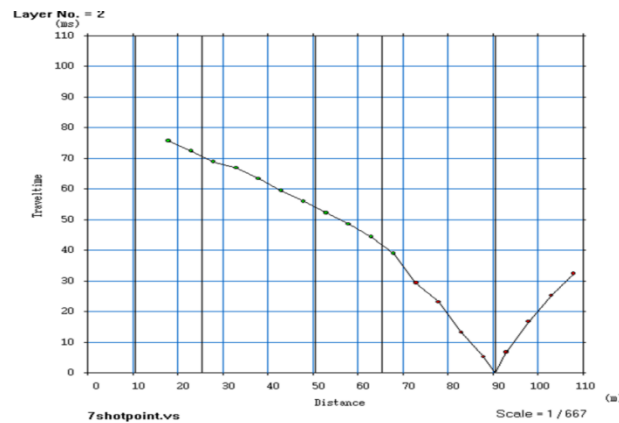
Figure 8. Travel time selected for PSO joint inversion algorithm.

Figure 9. S-wave structure obtained from experimental dataset using PSO joint inversion of ReMi and seismic refraction data (PSO joint Inv.), PSO inversion of ReMi data (PSO), and NSGA-II algorithm in joint inversion of ReMi and seismic refraction data (NSGA-II).
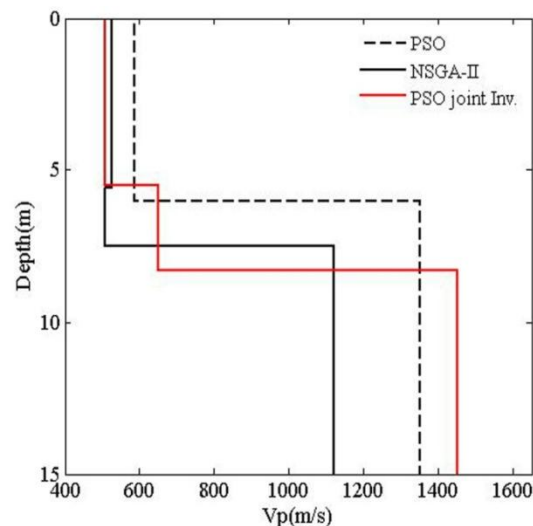
Figure 10. V$_P$ structure obtained from experimental dataset using PSO joint inversion of ReMi and seismic refraction data (PSO joint Inv.), PSO single inversion of seismic refraction data (PSO) and NSGA-II algorithm in joint inversion of ReMi and seismic refraction data (NSGA-II).

3. Discussion

Surface wave studies and seismic refraction technique are two main seismic methods in engineering geology and geotechnical studies. The surface wave dispersion analysis is an appropriate tool for a near-surface seismic characterization. However, the main problem is related to the non-uniqueness of the nature of the dispersion curve inversion. To overcome this problem, we need a careful strategy for the inversion of the dispersion curve. On the other hand, the seismic refraction studies also suffer from the hidden layer and non-uniqueness of the solution.

PSO algorithm is one of the global optimization methods that belong to a group of metaheuristic searching algorithm. In the proposed method, the refraction microtremor and seismic refraction data was concurrently inverted. This method was investigated by means of two synthetic datasets, and also by a real dataset. The PSO joint inversion algorithm was compared with the PSO single inversion and NSGA-II algorithm. Our findings show that the PSO joint inversion used in estimating the V$_S$ and thickness of the layers is more accurate than the PSO single inversion algorithm. Also the PSO joint inversion is more accurate, easier, and faster than NSGA-II. For more probe, the PSO joint inversion was investigated by the actual dataset performed in a part of Tabriz city in the NW of Iran. The results obtained show that the studied area is composed of two main layers. The first layer is made up of a soil consisting of alluvium and sandy clay soil, the intermediate layer is a mixture of clay and sand with moisture, and the last layer is made up of clay soil and Tuff.

4. Conclusions

Shear-wave velocity (V_S) is the main parameter for site characterization in geotechnical engineering. However, dispersion curve inversion is challenging for most inversion methods due to its high non-linearity and mixed-determined trait. In order to overcome these problems, in this study, a joint inversion strategy was proposed based on the particle swarm optimization (PSO) algorithm.

Therefore, in processing the geophysical data that suffer from non-uniqueness, especially when dealing with field datasets (necessarily including a variable amount of noise) by joint inversion, the final results appeared to be quite robust. The proposed PSO joint inversion algorithm is a high-performance approach in the joint inversion of the seismic data.

References

[1]. Foti, S., Sambuelli, L., Socco, V.L. and Strobbia, C. (2003). Experiments of joint acquisition of seismic refraction and surface wave data. Near Surface Geophysics. 3: 119-129.

[2]. Stephenson, W. J., Louie, J. N., Pullammanappallil, S., Williams, R.A. and Odum, J. K. (2005). Blind Shear-Wave Velocity Comparison of ReMi and MASW Results with Boreholes to 200m in Santa Clara Valley. Implications for Earthquake Ground-Motion Assessment. Bulletin of the Seismological Society of America. 95: 2506-2516.

[3]. Chavez-Garcia, F.J. and Kang, T-S. (2014). Lateral Heterogeneities and Microtremors: Limitations of HVSR and SPAC Based Studies for Site Response. Engineering Geology, doi: 10.1016/j.

[4]. Mahajan, A.K., Mundepi, A.K., Chauhan, N., Jasrotia, A.S., Rai, N. and Gachhayat, T.K. (2012). Active seismic and passive microtremor HVSR for assessing site effects in Jammu city, NW Himalaya, India, A case study. Journal of Applied Geophysics. 77: 51-62.

[5]. Louie, J.N. (2001). Faster, better: shear wave velocity to 100 meters depth from refraction Microtremor arrays. Bull. Seism. Soc. Am. 91: 347-364.

[6]. Rucker, M.L. (2003). Applying the refraction microtremor (ReMi) shear wave technique to geotechnical characterization . Proc. In. Conf. of the third international conference on the application of geophysical methodologies and NDT to transportation and infrastructure (Florida). 8-12.

[7]. Hering, A., Misiek, R., Gyulai, A., Ormos, T., Dobroka, M. and Dresen, L. (1995). A joint inversion algorithm to process geoelectric and sutface wave seismic data, Part 1: basic ideas. Geophysical Prospecting. 43: 135-156.

[8]. Dal Moro, G. (2008). V_S and V_P vertical profiling via joint inversion of Rayleigh waves and refraction travel times by means of bi-objective evolutionary algorithm. Journal of Applied Geophysics. 66: 15-24.

[9]. Fernández Martínez, J.L., García Gonzalo, E., Fernández Álvarez, J.P., Kuzma, H.A. and Menéndez Pérez, C.O. (2010). PSO: a powerful algorithm to solve geophysical inverse problems: application to a 1D-DC resistivity case. J. of Applied Geophysics. 71: 13-25.

[10]. Pekşen, E., Yas, T.A., Kayman, Y. and Özkan, C. (2011). Application of particle swarm optimization on self-potential data. Journal of Applied Geophysics. 75(2): 305-318.

[11]. Poormirzaee, R., Hamidzadeh, R.M. and Zarean, A. (2014). Inversion Seismic Refraction Data using Particle Swarm Optimization: a Case Study of Tabriz, Iran. Arabian Journal of Geosciences, DOI: 10.1007/s12517-014-1662-x.

[12]. Zarean, A., Mirzaei, N. and Mirzaei, M. (2015). Applying MPSO for Building Shear Wave Velocity Models from Microtremor Rayleigh-wave Dispersion Curves, Journal of Seismic Exploration. 24 (1): In-Press

[13]. Kennedy, J., Eberhart, R.C. (1995). Particle Swarm Optimization. Proceedings of IEEE International Conference on Neural Networks (Perth, Australia), Piscataway. 1942-1948.

[14]. Yang, X.S. (2010). Engineering Optimization an Introduction with Metaheuristic Applications John Wiley & Sons, 19-22.

[15]. Shi, Y. and Eberhart, R.C. (1998). A modified particle swarm optimizer. Proceedings of the IEEE International Conference on Evolutionary Computation, Piscataway, NJ: IEEE Press. 69-73.

[16]. Evers, G.I. (2009). An Automatic Regrouping Mechanism to Deal with Stagnation in Particle Swarm Optimization. Thesis for the degree of Master of Science university of Texas-pan American.

[17]. Clerc, M. (1999). The swarm and the queen: towards a deterministic and adaptive particle swarm optimization In: Angeline P J, Michalewicz Z, Schoenauer M, Yao X, Zalzala A (Eds.) Proc. of the Congress of Evolutionary Computation IEEE Press USA. 1951-1957.

[18]. Fernández Martínez, J.L., García Gonzalo, E., Fernández Muñiz, Z., Mariethoz, G. and Mukerji, T. (2010). Posterior sampling using particle swarm optimizers and model reduction techniques. International Journal of Applied Evolutionary Computation. 1(3): 27-48.

[19]. Wei, J. and Wang, Y. (2006). A dynamical particle swarm algorithm with dimension mutation. J Comput Sci Netw Secur. 6(7): 12-19.

[20]. Schutte, J.F. and Groenwold, A.A. (2005). A study of global optimization using particle swarms. Journal of Global Optimization. 31: 93-108.

[21]. Carlisle, A. and Dozier, G. (2001). An off-the-shelf PSO. Proc.of the 2001 Workshop On particle Swarm Optimization Indianapolis USA. 1-6.

[22]. Trelea, I.C. (2003). The particle swarm optimization algorithm: Convergence analysis and parameter selection. Information Processing Letters. 85: 317-325.

[23]. Clerc, M.A. and Kennedy, J. (2002). The particle swarm-explosion, stability, and convergence in a multidimensional complex space IEEE Transactions on Evolutionary Computation. 6 (1): 58-73.

[24]. Cha, Y.H., Kang, J.S. and Jo. C.H. (2006). Application of linear-array microtremor surveys for rock mass classification in urban tunnel design Exploration. Geophysics. 37: 108-113.

[25]. Kearey, P., Brooks, M. and Hill, I. (2002). An Introduction to Geophysical Exploration, Blackwell, Oxford.

[26]. Coccia, S., Del. Gaudio, V., Venisti, N. and Wasowski, N. (2010). Application of Refraction Microtremor (ReMi) technique for determination of 1-D shear wave velocity in a landslide area. J. of Applied Geophysics. 71: 71-89.

[27]. Panzera, F. and Lombardo, G. (2013). Seismic property characterization of lithotypes cropping out in the Siracusa urban area, Italy. Engineering Geology. 153: 12-24.

[28]. Poormirzaee, R. and Hamidzadeh, R.M. (2014). Determination of S-Wave structure via Refraction Microtremor Technique in Urban Area: a Case Study. Journal of Tethys. 2 (4): 347-356.

[29]. Scott, J. B., Clark, M., Rennie, T., Pancha, A., Park, H. and Louie, J.N. (2004). A Shallow Shear-Wave Velocity Transect across the Reno, Nevada, Area Basin. Bulletin of the Seismological Society of America. 94: 2222-2228.

[30]. Xia, J., Miller, R.D. and Park, C.B. (1999). Estimation of near-surface shear-wave velocity by inversion of Rayleigh waves. Geophysics. 64: 691-700.

[31]. Gardner, G.F., Gardner, L.W. and Gregory, A.R. (1974). Formation velocity and density the diagnostic basic for stratigraphic trap. Geophysics, 39: 770-780.

[32]. Herrmann, R.B. (1987). Computer Programs in Seismology St Louis University.

[33]. Poormirzaee, R., Hamidzadeh, R.M. and Zarean, A. (2014). PSO: a powerful and fast intelligence optimization method in processing of passive geophysical data, Proc. International Conference on Swarm Intelligence Based Optimization, Mulhouse, France. 12-19.

[34]. Deb, K., Agrawal, S., Pratab, A. and Meyarivan, T. (2000). A fast elitist nondominated sorting genetic algorithm for multi-objective optimization:NSGA-II. In Proc. Parallel Problem Solving From Nature VI Conf. 849-858.

[35]. Srinivas, N. and Deb, K. (1994). Multiobjective optimization using nondominated sorting in genetic algorithms. Evol. Comput. 2 (3): 221-248.

[36]. Coello Coello, C.A., Pulido, G.T. and Lechuga, M.A. (2004). Handling Multiple Objectives With Particle Swarm Optimization, IEEE Transactions On Evolutionary Computation. 8(3): 23-38.

[37]. SeisImager/SW Manual. (2009). Windows Software for Analysis of Surface Waves. Version 3.0, http://www.geometrics.com.

[38]. Golpasand, M.B., Nikudel, M.R. and Uromeihy, A. (2013). Predicting the occurrence of mixed face conditions in tunnel route of Line 2 Tabriz metro, Tabriz, Iran. In: Wu, F. and Qi, S., (ed) Global View of Engineering Geology and the Environment. Taylor & Francis Group, London.

وارون همزمان منحنی پاشش امواج میکروترمور و امواج انکساری با استفاده از بهینه‌سازی الگوریتم ازدحام ذرات

احمد زارعان[۱]* و راشد پور میرزائی[۲]

۱- گروه مهندسی عمران، واحد شبستر، دانشگاه آزاد اسلامی، ایران

۲- گروه مهندسی معدن و مواد، دانشگاه صنعتی ارومیه، ایران

* نویسنده مسئول مکاتبات: a.zarean@iaushab.ac.ir

چکیده:

مطالعه و مدل‌سازی ویژگی‌های سرعتی مناطق نزدیک سطح زمین به دلیل ارتباط مستقیم آن با تأسیسات شهری واقع بر روی آن، از لحاظ ژئوتکنیکی و مهندسی زلزله از اهمیت خاصی برخوردار است. در سال‌های اخیر میکروترمور شکست مرزی (ReMi) برای تخمین منحنی‌های پاشش و در نهایت مدل‌سازی سرعت موج برشی، به دلیل هزینه پائین و سرعت بالای برداشت داده‌ها مورد استقبال قرار گرفته است؛ اما مشکل اساسی در پردازش این داده‌ها وارون‌سازی منحنی پاشش جهت تخمین سرعت امواج برشی است. در مقاله حاضر سعی شده است با پیشنهاد وارون‌سازی همزمان امواج ReMi (امواج ریلی) و امواج انکساری (زمان سیر امواج) با روش بهینه‌سازی الگوریتم ازدحام ذرات، تخمینی از ساختار سرعت موج برشی ارائه شود. برنامه الگوریتم مذکور در محیط متلب نوشته شده است. روش پیشنهاد شده در ابتدا به‌وسیله مدل‌های مصنوعی مورد ارزیابی قرار گرفت و در ادامه برای ارزیابی بیشتر روی داده‌های تجربی اعمال شد. بدین منظور یک ایستگاه در تبریز برداشت شد. نتایج وارون‌سازی به‌دست آمده در مورد مدل‌های مصنوعی و هم داده‌های تجربی، بیانگر عملکرد قابل‌قبول الگوریتم پیشنهاد شده، به‌عنوان یک روش مؤثر در وارون‌سازی همزمان داده‌های ژئوفیزیکی، در مقایسه با سایر روش‌های مرسوم است. این الگوریتم یک راهکار مناسب در کاهش عدم یکتایی نتایج وارون‌سازی است.

کلمات کلیدی: سرعت موج برشی، وارون‌سازی همزمان، میکروترمور انکساری، الگوریتم ازدحام ذرات، زمان رسید.